- Technical Paper -

SHEAR FAILURE MECHANISM OF EXTERNALLY PRESTRESSED CONCRETE BEAMS CONSIDERING THE EFFECTIVE PRESTRESS

Chunyakom SIVALEEPUNTH[*1], Junichiro NIWA[*2], Satoshi TAMURA[*3] and Yuzuru HAMADA[*4]

ABSTRACT

This paper describes the results of an experimental study in order to investigate the shear failure mechanism of externally prestressed concrete beams by considering the effect of compressive stress in concrete due to prestress. The test results have shown that the beams having higher compressive stress provide higher shear carrying capacity and flatter inclination angle of diagonal cracks. The experimental results are also compared with the simplified truss model. It is found that the simplified truss model cannot predict the experimental results. The modification of this model is required for such beams.

Keywords: prestressed concrete, shear carrying capacity, external tendon, effective prestress, diagonal crack angle, simplified truss model

1. INTRODUCTION

As an innovative technology, externally prestressed concrete beams, in which the prestressing tendons are placed outside the concrete section and transfer the load to the concrete through end anchorages and deviators, have been recognized as an effective method for the modern construction of segmental box girder bridges and in the strengthening and rehabilitation of existing structures. By strengthening, the mode of failure may change from the previous expectation (i.e. the structures before strengthening), because the increase in flexural capacity is not always accompanied by an equivalent increase in shear capacity [1].

In conventional prestressed concrete slender beams (i.e. beams prestressed with bonded tendons), where the shear span to effective depth ratio, a/d, is greater than or equal to 2.5, most of them are found to fail in shear compressive mode of failure. Lertsamattiyakul [2] conducted the parametric study by using the finite element method (FEM) and proposed the simplified truss model in order to evaluate the shear carrying capacity of prestressed concrete slender beams without transverse reinforcement. The influential parameters, such as lower fiber stress, upper fiber stress, etc., were found to have a significant effect on the change of the inclination of concentrated stress flow, which is a key to solve the problem of shear compression failure mode. The model was found to be able to predict the several experimental results of beams prestressed with bonded tendons very well. However, there is a doubt whether the model can solve the problem of externally prestressed concrete beams with and without transverse reinforcement.

This study was therefore carried out to investigate the deficiency in the prediction of shear capacity and the inclination of diagonal cracks with emphasis on the influences of compressive stress in upper and lower extreme fibers of concrete due to the effective prestress, and the amount of transverse reinforcements. The objectives of this study are to investigate the influence of compressive stress in concrete due to prestress and the amount of transverse reinforcements in externally prestressed concrete beams on the shear carrying capacity and the inclination of diagonal cracks, to examine the failure mechanisms of externally prestressed concrete beams from the experimental study with the simplified truss model [2], and to check the capability of the simplified truss model for externally prestressed concrete beams. This paper compared the shear carrying capacity from the test with the simplified truss model [2].

*1 PhD. Candidate, Graduate School of Civil Engineering, Tokyo Institute of Technology, JCI Member
*2 Prof., Dept. of Civil Engineering, Tokyo Institute of Technology, Dr. E., JCI Member
*3 Research Engineer, Research and Development Center, DPS Bridge Works Co., Ltd., JCI Member
*4 Manager, Research and Development Center, DPS Bridge Works Co., Ltd., Dr. E., JCI Member

2. LITERATURE REVIEWS

Due to the comprehensive explanation for the failure mechanism of basis prestressed concrete beams, the simplified truss model [2] is adopted in this study. The schematic diagram of the simplified truss model [2] for analyzing the shear carrying capacity of prestressed concrete beams without transverse reinforcement is illustrated in Fig. 1. The model consists of 7 nodes and 11 elements for flexural compression members, transverse tension members, diagonal compression members and flexural tension members. The model is fixed in X-direction at both nodes along the center line and in Y-direction at the support. The parameter m is used in the model to represent the inverse of concentration of stress flow slope, where $m = \cot\theta$ and θ is an angle of the concentration stress flow. From the parametric study of the prestressed concrete beams without transverse reinforcement, the equation for estimating the value of m can be expressed as the following:

$$m = 2.55(\sigma_m)^{-\frac{3}{5}\left(\frac{b_f}{b_w}\right)^{-1}} \left(\frac{a}{d}\right)^{\left(\frac{b_f}{b_w}\right)^{-\frac{1}{5}}} \left(\frac{b_f}{b_w}\right)^{-\frac{3}{5}} \left(\frac{f_c'}{100}\right)^{\frac{3}{5}} \quad (1)$$

in which
$$\sigma_m = \left(1 + 0.2\frac{\sigma_u}{\sigma_u + \sigma_l}\right)\sigma_l \quad (2)$$

where σ_u is the upper extreme fiber stress; σ_l is the lower extreme fiber stress; b_f is the width of flange; b_w is the width of web; a is the shear span length; d is the effective depth; f_c' is the compressive strength of concrete.

By considering the effects of bearing plates and effective depth, the values of the horizontal thickness in the vicinity area of a loading point, t_l, and support, t_s, are expressed in Eqs. (3) and (4).

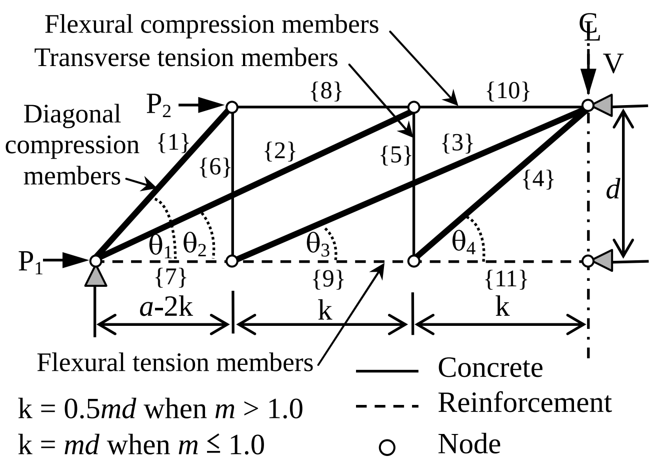

Fig. 1 Schematic diagram of the simplified truss model

For the cross sectional area of each compression member, A_i, i.e. {1}-{4}, it can be obtained as the value of t_s for {1} and {2} and the value of t_l for {3} and {4} multiplied with the width of web and its inclination.

$$t_1 = 2(r_l + 0.1d)\left(\frac{b_f}{b_w}\right)^{\frac{1}{5}} \quad (3)$$

$$t_s = 2(r_s + 0.1d)\left(\frac{b_f}{b_w}\right)^{\frac{1}{5}} \quad (4)$$

where r_l is the width of loading plate and r_s is the width of support plate.

The value of compression softening parameter, η, affected by the existence of cracks is also considered in order to compute the resisting capacity of each member, and can be simply expressed as in Eq. (5).

$$\eta = -0.3\left(\frac{f_c'}{100}\right) + 0.7 \quad (5)$$

The resistance capacity of each diagonal compression member, R_i, can be obtained from following expression.

$$R_i = \eta f_c' A_i \sin\theta_i \quad (6)$$

The member force of each member due to the external shear force can be determined based on Castigliano's second theorem. The redundant member force, X_i, can be obtained when the strain energy, U is minimized as summarized in Eqs. (7) and (8). The critical diagonal compression member can be determined when the ratio of F_i and R_i becomes the maximum and equal to 1.0.

$$\frac{\partial U}{\partial X_i} = 0 \quad (7)$$

$$\sum_{i=1}^{11}\left[F_i \frac{\partial F_i}{\partial X_i}\frac{L_i}{E_i A_i}\right] = 0 \quad (8)$$

where $\frac{\partial F_i}{\partial X_i}$ is the unit force, L_i and E_i are the length and stiffness of each member, respectively.

Although the simplified truss model is proven to provide simplicity and high accuracy (mean = 1.0; coefficient of variation = 0.13) in the prediction on shear carrying capacity of concrete beams prestressed with bonded prestressing bars without transverse reinforcement [2], it is not checked to extend this model to the externally prestressed concrete beams with and without transverse reinforcement, since the prestressing tendons in externally prestressed concrete beams are unbonded to the concrete, and when the beams are subjected to an externally applied load, the external tendons are free to move relative to the axis of the beams, defined as second order effects. This may cause the change of inclination of concentrated stress flow, θ.

3. TEST PROGRAMS

The test specimens consisted of four concrete beams prestressed with external tendons, with the same total length at 3.5 m, cross section dimensions and reinforcement details as shown in Fig. 2. The specimens were named as ns7, ns14, s7 and s14 as tabulated in Table 1. The main parameters in this experimental study were the compressive stress in concrete due to the prestress, and transverse reinforcements. The effective prestress was set as 500 N/mm^2 for specimens ns7 and s7 in order to generate the compressive stress in concrete at the upper extreme fiber, σ_u, and the lower extreme fiber, σ_l, as -1.5 N/mm^2 and 7.4 N/mm^2, respectively. For specimens ns14 and s14, 1000 N/mm^2 of effective prestress was introduced in order to obtain the compressive stress in concrete at the upper extreme fiber, σ_u, as -3.0 N/mm^2 and the lower extreme fiber, σ_l, as 14.9 N/mm^2. Vertical transverse reinforcements were used as shear reinforcement for specimens s7 and s14; however, for specimens ns7 and ns14, the transverse reinforcement was not provided in the test span in order to examine the shear contribution of concrete and prestressing force.

Table 1 Detail of test beams

Beams	Effective span length, L [mm]	Loading distance, L_d [mm]	Deviator spacing, S_d [mm]	Depth of tendon, d_{ps} [mm]	Area of internal steel bars, A_s [mm^2]	Area of external tendon, A_{ps} [mm^2]	Effective prestress, f_{pe} [N/mm^2]	Shear reinforce-ment ratio in web [%]
ns7	3200	400	1366.6	400	2026.8	416.8	487.2	0
ns14							962.4	0
s7							487.2	0.21
s14							932.3	0.21

Table 2 Mix proportion of concrete

W/C [%]	s/a [%]	W*1 [kg/m^3]	C*2 [kg/m^3]	S*3 [kg/m^3]	G*4 [kg/m^3]	SP*5 [kg/m^3]	AE*6 [kg/m^3]
35.5	38.5	143	403	690	1114	0.75	1.21

*1 Water
*2 Early High-strength Portland Cement, specific gravity = 3.14
*3 Fine aggregate, specific gravity = 2.60, F.M. = 2.73
*4 Coarse aggregate, specific gravity = 2.63, F.M. = 6.68, G_{max} = 20mm
*5 Superplasticizer, specific gravity = 1.05
*6 Air-entraining agent, specific gravity = 1.02, 100 time dilute solution

Table 3 Mechanical properties of concrete from experiment

Beams	Compressive strength, f_c' [N/mm^2]	Tensile strength, f_t [N/mm^2]	Elastic modulus, E_c [kN/mm^2]
ns7	53.6	4.1	32.5
ns14	55.8	4.2	31.1
s7	57.4	3.7	31.8
s14	58.6	4.0	32.2

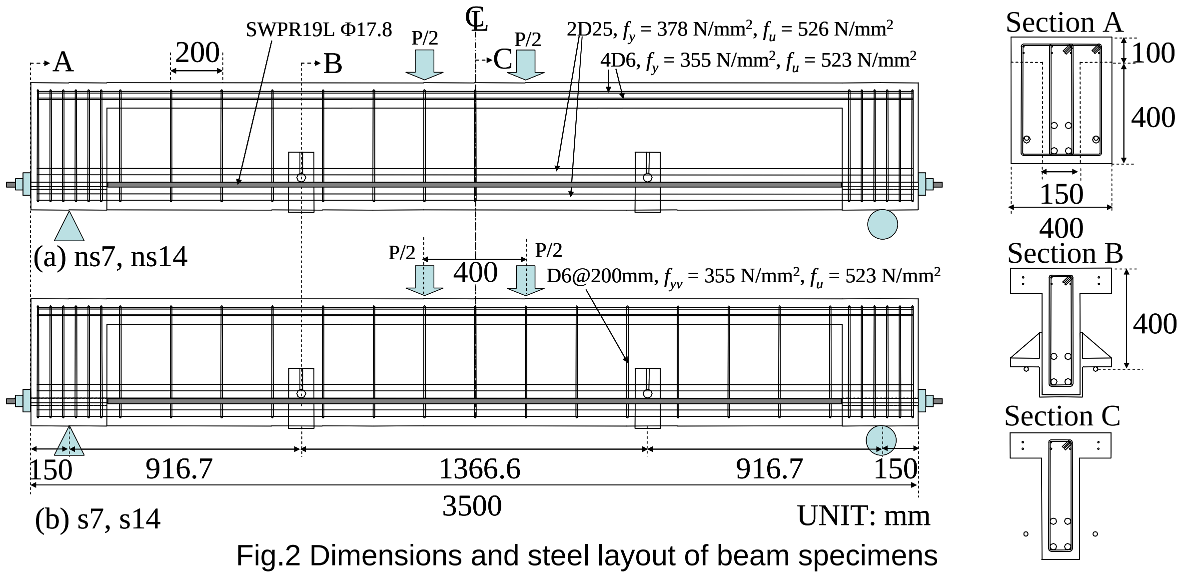

Fig.2 Dimensions and steel layout of beam specimens

3.1 Materials

(1) Reinforcements

In all specimens, the internal longitudinal tensile reinforcement consisted of four deformed steel bars with nominal diameter of 25 mm (A_s = 506.7 mm^2), which providing the reinforcement ratio ($\rho_w = A_s/b_wd$) as 4.07 %, including the area of external tendons, and eight deformed steel bars are for longitudinal compressive reinforcement with nominal diameter of 6 mm (A_s' = 31.67 mm^2). Their average yield strength, f_y, is 378 N/mm^2 and 355 N/mm^2, and average tensile strength, f_u, is 526 N/mm^2 and 523 N/mm^2, respectively. For specimens s7 and s14, transverse reinforcement with a nominal diameter of 6 mm (A_v = 63.34 mm^2) and with yield strength, f_{yv}, of 355 N/mm^2 was provided in a web throughout the length of beams with the spacing, s, of 200 mm. The shear reinforcement ratio (A_v/b_ws) was 0.21 %.

(2) Concrete

The concrete has a mix proportion as summarized in Table 2. The water cement ratio was 35.5% and the design cylindrical compressive strength of concrete, f_c', was 50 N/mm^2 at 7 days. The actual strength of concrete in each batch of casting was measured on the day of testing as tabulated in Table 3.

(3) External tendons

Two straight 19-wire prestressing tendons with a nominal diameter of 17.8 mm (A_{ps} = 208.4 mm^2) were prepared for each specimen as external tendons. The yield strength, f_{py}, the tensile strength, f_{pu}, and the modulus of elasticity of external tendons, E_{ps}, were 1694 N/mm^2, 1934 N/mm^2 and 191.9 kN/mm^2, respectively.

3.2 Experimental Procedure

Before testing, the beam specimens were prestressed using symmetrically arranged external tendons on both sides of the section of externally prestressed concrete beams deviated at 916.7 mm from the supports by two deviators and anchored at the ends of beams. Teflon sheets were inserted between a specimen and supports and between tendons and deviators for reducing the friction. Three electrical strain gauges were placed on each tendon at the same section at the midspan of the beam. The strain of the prestressing tendon was taken as the average value of three measured locations.

All beams had straight tendon profiles, with a depth of 400 mm at the midspan section. The tendons were stressed to about 0.25f_{pu} for ns7 and s7, and 0.5f_{pu} for ns14 and s14 as illustrated as the effective prestress, f_{pe}, in Table 1. Each beam was instrumented to measure and monitor deflections at the midspan and deviators, crack width, prestressing force in external tendons, and strains of concrete, steel and tendon. The beams were simply supported over a span of 3.2 m and four-point symmetrical loading with a distance between loading points of 400 mm was provided. The shear span was set as 1.4 m, and the effective depth was 400 mm (i.e. shear span to effective depth ratio, a/d, was 3.5). The 150 mm width of loading and support plates were used in the test.

4. RESULTS AND DISCUSSION

4.1 Cracking Behavior

The crack patterns of all specimens were demonstrated in Fig 3. Flexural cracks were firstly observed in the flexural span between loading points, where the maximum moment region is. As the load increased, several new flexural cracks were developed in both shear spans, and these flexural cracks started to incline forming diagonal cracks. These diagonal cracks increased significantly in width and propagated upward to the compression zone of beams. These cracks were generally defined as flexural shear cracks. Although the diagonal crack formed, the beams could resist more loads. The loading was continued until the peak load of beams. For the specimens ns7 and ns14, which did not have any transverse reinforcement in the test span, a new diagonal crack penetrating from the loading point to the support was suddenly observed at the peak load, and the load suddenly decreased. However, in the specimens s7 and s14, which had transverse reinforcements, the primary diagonal crack gradually increased in width and failed at the peak load. The stress flow inside the beams exhibited as the compression arch to resist the shear force and failed in the shear compressive mode of failure, even though the concrete strain at the top flange was small as shown in Table 4. The inclination of diagonal crack, β, was measured by taking average values of crack angles measured from several locations of primary diagonal crack and illustrated in Fig 3. It is found that the inclinations of diagonal cracks become flatter in the beams with higher value of compressive extreme fiber stress, and become slightly steeper by introducing vertical shear reinforcements.

4.2 Load-deflection Characteristics

The responses of applied load versus deflection of beams are illustrated in Fig. 4. The summary of measured resistances of specimens from the cracking to the peak load together with the midspan deformation, stress in tendon at the

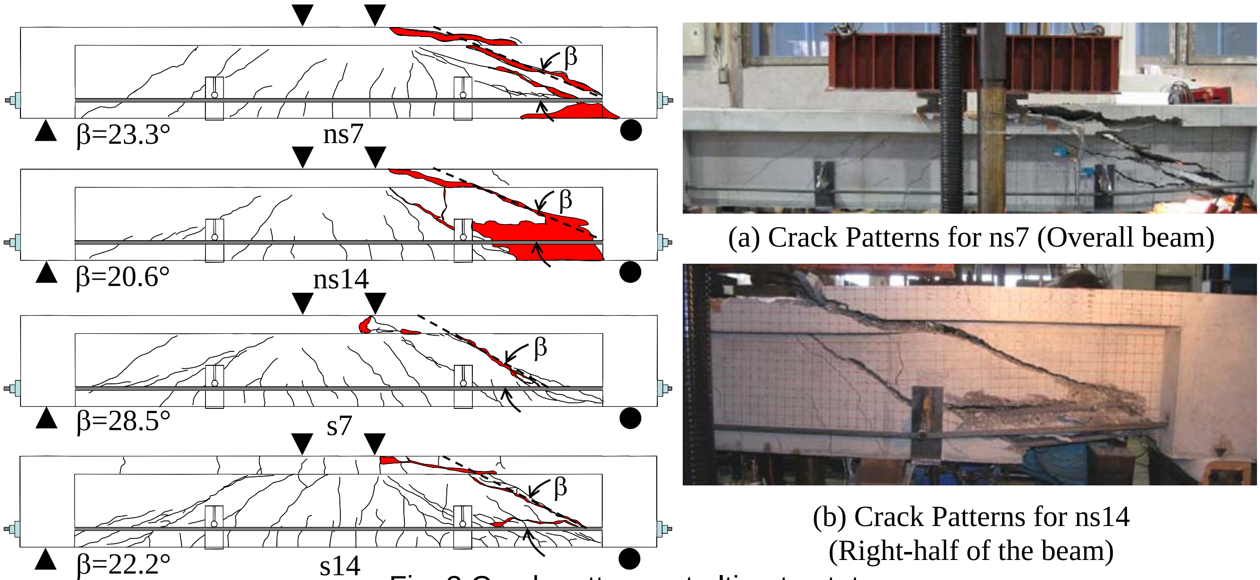

(a) Crack Patterns for ns7 (Overall beam)

(b) Crack Patterns for ns14
(Right-half of the beam)

Fig. 3 Crack patterns at ultimate state

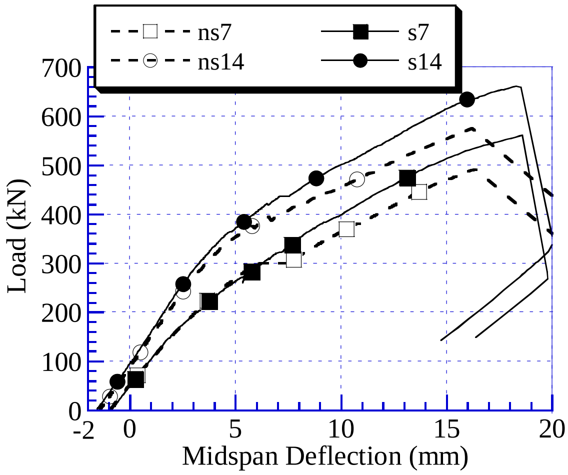

Fig. 4 Load-deflection responses

Table 4 Summary of experimental results

Beams	ε_u *1	f_{ps} *2	P_{crack} *3	$P_{dia.}$ *4	$P_{u,EXP}$ *5	δ_u *6	d_{pu} *7
ns7	1437	658.2	193.5	303.4	491.2	16.4	396.9
ns14	1701	1144.1	295.5	373.1	574.8	16.2	397.5
s7	1457	698.2	192.6	379.2	560.6	18.6	396.8
s14	1920	1122.5	296.4	436.4	660.6	18.3	396.8

*1 Concrete strain of peak resistance at the top flange [$*10^{-6}$]
*2 Stress in tendon of peak resistance [N/mm^2]
*3 Load of first flexural crack [kN]
*4 Load of first diagonal crack [kN]
*5 Load of peak resistance [kN], $P_{u,EXP} = 2V_{u,EXP}$
*6 Midspan deflection at peak resistance [mm]
*7 Tendon depth of peak resistance [mm]

peak and tendon depth at the peak are tabulated in Table 4. In the beginning, the beams behaved as the linear elastic body until the first flexural crack between loading points occurred that reduced the beam stiffness. It should be noted that by increasing the lower extreme fiber stress, σ_l, from 7.4 N/mm^2 to 14.9 N/mm^2, it makes the load at the first flexural crack increase for 50.7%. The loading was continued until the diagonal crack appeared, which caused the loads slightly dropped and changed the beam stiffness for specimens ns7 and ns14, which did not have any transverse reinforcement in the test span. On the other hand, for specimens s7 and s14, which had transverse reinforcements, the loading was smoothly continued, and only the change in the beam stiffness could be observed when the diagonal crack was appeared. It is interesting to notice that the loading resistances at the first diagonal crack of ns14 (without transverse reinforcement, σ_l = 14.9 N/mm^2) and s7 (with transverse reinforcement, σ_l = 7.4 N/mm^2) are almost the same, even though there was no transverse reinforcement in the specimen ns14, which means that the lower extreme fiber stress in concrete, σ_l, has a significant impact to resist the shear force. And then the loads gradually increased again until the peak resistance. From the experiment, the shear contribution of vertical transverse reinforcement, V_s (= V_u- V_{pc}, where V_u is the shear carrying capacity from specimens with stirrups and V_{pc} is the shear contribution of concrete and prestressing force from specimens without stirrup), can be obtained as 34.7 kN and 42.9 kN for s7 and s14, respectively. However, the shear contribution of vertical transverse reinforcement from computation ($V_s = A_v f_{yv} z/s$) can be obtained as 30.1 kN. Therefore, it can be concluded that the lower fiber stress, σ_l, also affects the shear contribution of transverse reinforcement due to the change of the inclination of diagonal crack. The second order effects can be neglected in the case of shear failure mode, since from the experimental results, the tendon depth at the peak changed only about 0.75% from the initial tendon depth. The stress increment in tendons, Δf_{ps} (=f_{ps}-f_{pe}), did not increase as much as in the case of flexural problem [3], because the deflection of such beams, which failed in shear, is not much.

5. COMPARISON WITH THE SIMPLIFIED TRUSS MODEL

The applicability of the simplified truss model, Eqs. (1)-(8), on the externally prestressed concrete beams without transverse reinforcement was inspected with the experimental results by focusing on the comparison of failed members of the predicted results and the crack patterns in Fig. 3 as illustrated in Fig. 5, and the comparison of shear carrying capacity of the beams as tabulated in Table 5. It is apparent that the calculated results provide the well-predicted results compared with the test results for specimen ns7, but the failed member obtained from the prediction is not the same as obtained from the test. From the test, the member {2} was a critical member, but in the simplified truss model, instead of member {2}, member {3} is a critical member as shown in Fig. 5. However, from Table 5, it can be observed that the member {2} almost concurrently failed with the member {3}. On the other hand, in specimen ns14, the prediction of shear carrying capacity is quite conservative, but the prediction of failed member, member {2}, is well predicted. This may be due to the fact that the prestressing tendons in externally prestressed concrete beams were unbonded to the concrete; therefore, the inverse of slope of concentrated stress flow, *m*, Eq. (1), may not be able to be estimated from the model. The modification of parameter *m* is required in order to predict the shear carrying capacity of externally prestressed concrete beams.

For the specimens s7 and s14, in which transverse reinforcements were provided, the inclination of diagonal crack becomes steeper, and the shear carrying capacity was also higher according to the experimental results in Fig. 3 and Table 4. Therefore, from these results, it can be concluded that the inclination of concentrated stress flow, θ, needs to be modified in order to obtain a reliable inclination for beams with transverse reinforcements.

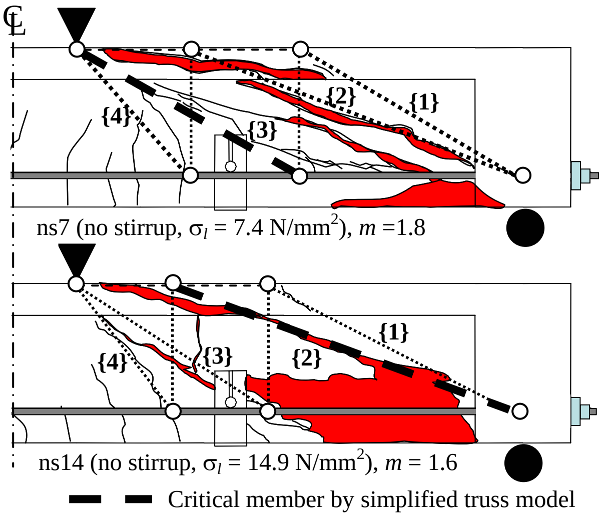

Fig. 5 Critical members and crack patterns

Table 5 Analytical results in each member

Member No.	ns7*1			ns14*2		
	F_i (kN)	R_i (kN)	F_i/R_i	F_i (kN)	R_i (kN)	F_i/R_i
1	-232.2	-508.5	0.46	-270.4	-432.9	0.62
2	-244.8	-257.0	0.95	-245.4	-245.5	1.00
3	-239.3	-239.4	1.00	-229.7	-300.0	0.77
4	-117.5	-557.8	0.21	-107.4	-640.5	0.17

*1 $V_{u,CAL}$ = 204.6 kN; $V_{u,CAL}/V_{u,EXP}$ = 0.83
*2 $V_{u,CAL}$ = 208.6 kN; $V_{u,CAL}/V_{u,EXP}$ = 0.73

6. CONCLUSIONS

(1) By increasing the lower fiber stress in concrete, the shear carrying capacity also increases, and the diagonal crack inclination becomes flatter. However, if the transverse reinforcements are provided, the diagonal crack inclination becomes steeper.
(2) From both experimental and calculated results of externally prestressed concrete beams, the shear compression failure is determined to cause the crushing of web concrete.
(3) The modification of the simplified truss model is required in order to obtain higher accuracy.

ACKNOWLEDGEMENT

Sincere gratitude is expressed to Dr. Bui Khac Diep, postdoctoral researcher, Department of Civil Engineering, Tokyo Institute of Technology for his assistance in conducting the experiment.

REFERENCES

[1] Tan, K.H. and Tjandra R.A.: Shear Deficiency in Reinforced Concrete Continuous Beams Strengthened with External Tendons, ACI Structural Journal, Vol. 100, No. 5, pp. 565-572, 2003
[2] Lertsamattiyakul, M.: Simplified Truss Model for Shear Carrying Capacity of Prestressed Concrete Members, PhD thesis, Tokyo Institute of Technology, 2005
[3] Sivaleepunth, C., Niwa, J., Tamura, S. and Hamada, Y.: Flexural Behavior of Externally Prestressed Concrete Beams by Considering Loading Application, Proceedings of the JCI, Vol. 27, No. 2, pp. 553-558, 2005